VPS VIBRATIONS IN PHYSICAL SYSTEMS

DOI: 10.21008/j.0860-6897.2023.1.20
Vibrations in Physical Systems, 2023, 34(1), 2023120

Numerical simulation of fundamental elastic wave modes coupling in composite plates

Marek BARSKI, Adam STAWIARSKI, Małgorzata CHWAŁ, Marcin AUGUSTYN

Cracow University of Technology, al. Jana Pawła II 37, 31-864 Kraków, Poland

Corresponding author: Marek BARSKI, email: marek.barski@pk.edu.pl

Abstract In the case of the piezoelectric actuators of the cube-shaped installed symmetrically and perfectly bonded on both external surfaces of the plate-like structures, the symmetric and shear horizontal elastic wave modes are excited at the same time. The current work concerns the numerical simulation of the coupling of the above-mentioned elastic wave modes in a composite plate of angle ply configuration. In the first step, the dispersion curves for all studied composite configurations are estimated. Next, for the arbitrary chosen fixed frequency of the excitation, finite element simulations are performed. As a result of these simulations, the group velocities of the observed elastic modes are estimated. Next, the appropriate wave modes are identified by the comparison of the group velocities obtained from the analysis of the dispersion curves and from the simulations. In the cases for which the identification is possible, a good agreement between analytical and simulation results is observed.

Keywords: shear horizontal wave mode, symmetric wave mode, dispersion curves, finite element method.

1. Introduction

The phenomenon of the propagation of the elastic wave in composite structures is nowadays frequently used as a fundament of different structural health monitoring (SHM) systems [1-2]. The crucial impact on the effectiveness of such systems possesses the way how the elastic waves are excited and further propagate through the interrogated structure. In order to detect the specified types of damage, the particular elastic wave mode has to be excited. It seems that the simplest solution is to use the fundamental anti-symmetric mode [3]. However, in some cases, the most effective way is to apply the fundamental symmetric wave mode. The important advantage of this approach is that for relatively small excitation frequency this mode is almost not dispersive. The above fact essentially simplifies the process of interpretation of the registered response of the analysed structure, especially when the SHM system works according to the pulse-echo configuration. In these kinds of systems, the main problem concerns the way how to excite selectively the symmetric wave mode. It seems that the most effective way is to install identical piezoelectric elements on both sides of the interrogated structure (for example composite plate) and excite them by the identical electric signals. However, in the case of perfectly bonded cube-shaped sensors, as it will be shown further, besides the expected symmetric wave mode the shear horizontal wave mode is also excited. Moreover, for some composite configurations, these modes due to similar values of the phase and group velocity overlap each other. This fact radically hinders the appropriate design of the effective SHM system.

Generally, the first step of the design process of the SHM system is to determine the dispersion characteristic of the composite structure, which will be analysed with the use of elastic waves, so-called dispersion curves. It should be stressed here that in the case of multi-layered composite materials it is a challenging task. The most frequently used methods are so-called matrix methods, namely the transfer matrix method (TMM) [4-7], the global matrix method (GMM) [8], or the stiffness matrix method (SMM) [9-10]. According to the experience of authors [11-13], the last mentioned method seems to be the most effective and robust. Moreover, in comparison with the other mentioned matrix methods is unconditionally numerically stable. In order to automatically generate the dispersion curves for the arbitrarily chosen configuration of the composite material, our own software, *DisperseWin*, has been developed. This software uses the SMM approach.

Having determined the dynamic properties of the composite structure, next the phenomenon of the selected elastic wave modes propagation has to be studied. Such an analysis could be performed experimentally or by carrying out specific numerical simulations. The main disadvantage of the first approach is that it requires the use of very expensive measurement equipment and the preparation of a real

model of the structure. The second approach seems to be very effective in the preliminary stage of the SHM system design. Most frequently, the standard software (ANSYS, ABAQUS, LS-DYNA) [14, 15] based on the finite element (FE) method is used. However, some other methods are also developed [16-18]. As a result of the numerical simulation, not only the dynamic response of the structure in the selected points are registered but also the shape of the wavefront of the elastic wave can be studied as the function of time.

In the current work for the composite plate of the arbitrarily chosen configuration the dynamic properties are determined and next several numerical simulations are performed in order to study the coupling of the fundamental symmetric mode and the fundamental shear horizontal mode. The mentioned coupling is caused by the way how the elastic wave is excited. The particular wave modes are identified by the enveloped method or by the cross-correlation method.

2. Analysed composite plate

The dispersion curves are determined for the laminate made of carbon fibre/epoxy resin (fibres T300, matrix N5208). The mechanical properties of the layers are as follows: E_1 = 181 GPa, E_2=10.3 GPa, G_{12} = 7.17 GPa, ν_{12} = 0.28, and density ρ = 1.6 g/cm^3. The laminate consists of 8 layers of identical thickness, where t_i = 0.25 mm. Thus the total thickness of the composite material is t_c = 2 mm. It is assumed that the studied laminate is of the angle-ply configuration, namely $[\pm\theta]_4$, where θ denotes the angle between the fibres in a particular layer and the X_1 is the direction of the global coordinate system, which is shown in Fig. 1. The dispersion curves are determined for the following fibre orientation angles, namely θ = [0°, 5°, 15°, 25°, ... , 75°, 85°, 90°]. It should be noted the composites of fibre orientation angle θ = 0° and 90° are single-layer composite material. Moreover, it is assumed that the elastic wavefront propagates in the direction, which is perpendicular to the X_1 axis of the global Cartesian coordinate system.

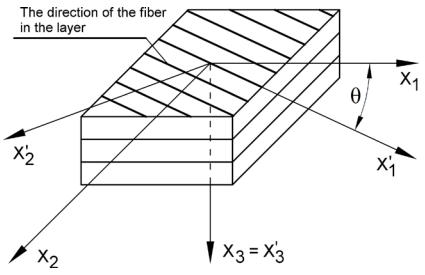

Figure 1. The layer (X'_1, X'_2, X'_3) and the global (X_1, X_2, X_3) Cartesian coordinate system for the studied carbon laminate, where the X_1 is the direction of the elastic wave propagation.

In Figure 2, there are shown the dispersion curves for the fundamental modes S0, A0, SH0, and the first higher mode H1. For clarity, the rest of the higher modes have been neglected. Together with the increasing value of the fibre orientation angle θ, the phase velocity of the fundamental symmetric mode S0 decreases. However, in the range of frequency limited by the occurrence of the first higher mode, the phase velocity of the mode S0 remains almost constant for all analysed cases. Moreover, for the angle θ = 55°, 65°, and 75° the phase velocity of the symmetric mode S0 is lower in comparison with the phase velocity of the fundamental shear horizontal mode SH0, which can be quite surprising. The dispersion curves, which describe the SH0 modes are no longer constant. Initially, the value of the phase velocity of SH0 mode increases, and at the fibre orientation angle, θ = 45° reaches the global maximum, where c = 5.5 km/s for the beginning frequency f = 0.005 MHz. The dispersion curves describing the fundamental antisymmetric wave mode A0 are not very sensitive to the variations of the fibre orientation angle θ. Finally, it is worth noting that the value of the frequency at which the first higher wave mode appears, varies also not significantly. The highest frequency is observed for the fibre orientation angle θ = 45° and the corresponding value of frequency f = 0.6 MHz. In Figure 3, there is depicted the phase c and group velocity c_g of the fundamental elastic wave modes as a function of the fibre orientation angle θ. Because of the fact that in further finite element simulations of the elastic wave propagation the central frequency of the excitation signal is f_c = 125 kHz. In Table 1 there are presented the values of the phase c and group c_g velocities for all studied laminate configurations for the assumed frequency value. It is worth noting that only in the case of the anti-symmetric fundamental wave mode A0 the value of the group velocity c_g is slightly greater in comparison with the value of the phase velocity c.

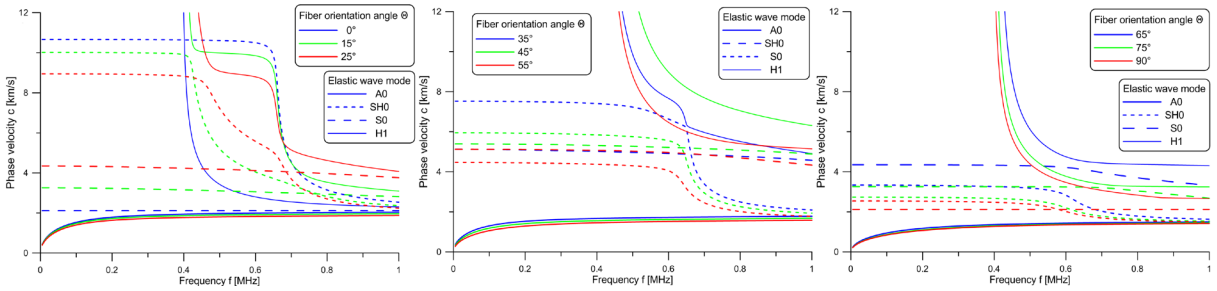

Figure 2. Dispersion curves generated for the studied set of composite configurations.

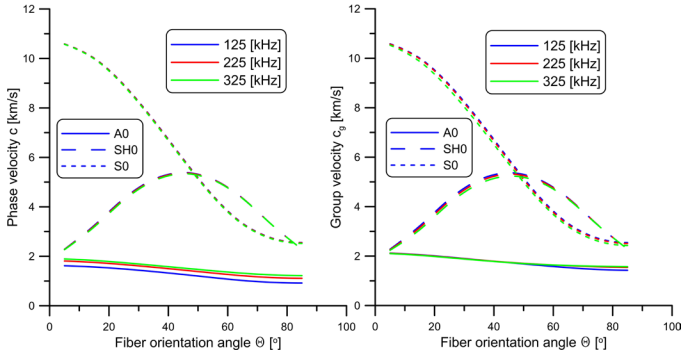

Figure 3. Phase c and group c_g velocities as a function of the fibre orientation angle θ.

Table 1. Phase c and group c_g [km/s] velocities of the fundamental modes, f = 125 [kHz].

Composite configuration	Mode A0		Mode SH0		Mode S0	
	c	c_g	c	c_g	c	c_g
$[\pm 5°]_4$	1.618	2.119	2.282	2.276	10.585	10.582
$[\pm 15°]_4$	1.567	2.054	3.247	3.219	10.012	10.006
$[\pm 25°]_4$	1.486	1.957	4.335	4.305	8.941	8.930
$[\pm 35°]_4$	1.383	1.846	5.109	5.085	7.517	7.501
$[\pm 45°]_4$	1.264	1.736	5.388	5.371	5.942	5.923
$[\pm 55°]_4$	1.138	1.631	5.118	5.108	4.460	4.443
$[\pm 65°]_4$	1.022	1.533	4.350	4.346	3.333	3.320
$[\pm 75°]_4$	0.946	1.459	3.262	3.261	2.732	2.723
$[\pm 85°]_4$	0.919	1.428	2.286	2.286	2.553	2.545

Due to the fact that the observed differences in the value of phase c and group c_g velocities for the fibre angle orientation θ = 0° and θ = 5° as well as θ = 85° and θ = 90° are almost identical thus the further analysis will be performed with the neglection the composite configuration where θ = 0°, 90°.

As can be observed, the value of phase c and group c_g velocity of the fundamental symmetric mode S0 monotonically decreases together with the increase of the fibre orientation angle. What should be stressed here, the curves obtained for different values of frequency are almost identical. For the fibre orientation θ = 48° the phase c and group c_g velocities of the symmetric mode, S0 are significantly lower in comparison with the corresponding quantities for the fundamental shear horizontal mode SH0. In the case of the fundamental shear horizontal wave mode SH0 the clear global maximum is observed for the value of fibre orientation angle θ = 45° and the corresponding maximal value of the phase velocity equals c = 5.5 km/s.

2. Finite element simulation

In all conducted simulation the input signal is excited by the two actuators of the cubic shape, which are perfectly installed in the same position on both external surfaces of the composite plate. In the FE simulations (ANSYS), they are modelled by the solid (volume) elements SOLID186. On the appropriate walls of these sensors acts the external pressure p, which causes the deformation of the sensors and, in consequence, excites the elastic wave. The value of the external pressure p varies according to a five-cycle sine wave (tone burst) modulated with the Hanning window of central frequency f_c = 125 kHz.

The composite plate is modelled with the use of four-nodes, rectangular-shaped, multi-layered shell elements SHELL181 (ANSYS). The transient FE analysis is performed according to Newmark's implicit schema. In order to obtain the appropriate accuracy of the numerical simulations, the element size and time step size has to satisfy the following conditions [16, 17]. The time step size Δt should be of the following value: $\Delta t = 1/(\varepsilon \cdot f_{max})$, where f_{max} is the highest frequency component of the excitation (input) signal, and $\varepsilon = 20$. The corresponding maximal element size l_e should be assumed as $l_e = \lambda_{min}/20$, where λ_{min} is the shortest wavelength component of the exciting elastic wave. Due to significant variations of the phase c and group velocity c_g of the fundamental elastic wave modes, especially symmetric S0, depending on the fibre orientation angle θ (see Tab. 1), the numerical simulations are carried out in two variants. It is necessary in order to fulfil the above-mentioned conditions concerning the optimal time step Δt and length of the finite element l_e. In the first variant the symmetric fundamental wave mode is identified and in the second the fundamental shear horizontal wave mode is identified.

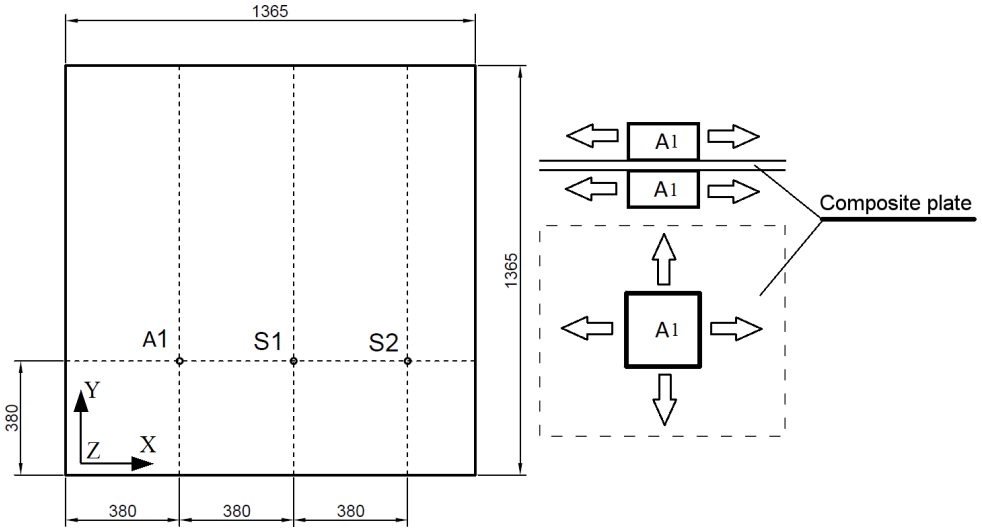

Figure 4. Model of the composite plate used for the simulation of fundamental symmetric wave mode S0: the geometrical dimensions with the location of sensors and the schematic view of the actuator and the way how the symmetric wave mode S0 is excited.

Table 2. Variable parameters of FE simulations of the propagation of the fundamental symmetric wave mode S0.

Laminate configuration	Wavelength λ_{S0} [mm]	Total time of simulation $t_c \cdot 10^{-4}$ [s]	Time step $\Delta t \cdot 10^{-7}$ [s]
$[\pm 5°]_4$	84.680	1.181	1.890
$[\pm 15°]_4$	80.094	1.249	1.999
$[\pm 25°]_4$	71.524	1.400	2.240
$[\pm 35°]_4$	60.136	1.666	2.666
$[\pm 45°]_4$	47.534	2.110	3.376
$[\pm 55°]_4$	40.941	2.447	3.915
$[\pm 65°]_4$	34.801	2.876	4.602
$[\pm 75°]_4$	26.096	3.833	6.133
$[\pm 85°]_4$	20.424	9.823	15.717

For the first variant the geometrical dimensions of the structure are shown in Fig. 4. The locations of the actuator A and sensors S1 and S2 are constant for all performed numerical experiments. The elastic wave is excited by actuator A and the dynamic response of the structure is registered by the sensors S1 and S2. All these sensors are laying along the line, which is parallel to the *X*-axis of the global Cartesian coordinate system. It is worth stressing here that the fibre orientation angle θ in the analysed composite material is also defined with respect to this axis. The considered composite plate is divided into the FE elements of square shape with edge length l_e = 3.5 mm (identical for all performed simulations). The actuators (installed

on both sides of the plate as depicted in Fig. 4) are modelled by four solid elements thus their geometrical dimensions are 7 × 7 × 3.5 mm. The time step Δt, and the total time of simulation t_c are changeable. They are set individually for each performed simulation. The only parameter, which is identical for all simulations is the total number of time steps n = 625. The values of the time step Δt, total times of simulations t_c, and the wavelength λ_{S0} with respect to the composite configuration are presented in Tab. 2.

The exemplary results of the simulation for the laminate of configuration $[\pm 5°]_4$ are presented in Fig. 5. As it can be observed there are two different wave modes. The strongly elongated elliptical wavefront can be considered as the fundamental symmetric mode S0. The elongation of the wavefront is in the direction of the *X*-axis of the global coordinate system. In this direction, the in-plane stiffness of the composite plate is the highest and, in consequence, the wave speed is also the highest. However, another approximately circular wavefront is also visible, which is localized around actuator A1. Taking into consideration the cubic shape of the actuator and the way how the elastic wave is excited, this additional wave can be considered as the fundamental shear horizontal wave mode SH0. In order to clearly identify this wave mode the special model of the actuator will be presented in the next section. Now it is worth noting the strong interaction between these two modes in the direction of the *Y*-axis of the global coordinate system. Unfortunately, this fact significantly impedes or even precludes correct distinguishing between the in-plane wave modes, namely the symmetric modes S and shear the horizontal modes SH and it also confirms that for the fibre orientation angle $\theta > 45°$ the phase c and group c_g velocity of these modes are very similar as it is shown in Fig. 3. The dynamic response of the studied plate (a component of displacement *UX*, and *UZ*) registered by the sensors S1 and S2 is presented in Fig. 6.

The estimation of the group velocity c_g for this variant of simulations is shown in Tab. 3. Both applied methods, namely the enveloped method (EMM) and the cross-correlation method (CCM), provides very accurate result in comparison with the theoretical values presented in Tab. 1. The error is about 1 %. In the case of the other studied laminate configurations, the accuracy is similar however, the value of the error increases. In the case of laminate configuration $[\pm 45°]_4$ the wave velocities, c and c_g, are comparable (Tab. 1) and the symmetric wave mode S0 and the shear horizontal wave mode SH0 overlap almost perfectly with each other, and the mode identification by comparison of the group velocities is still possible.

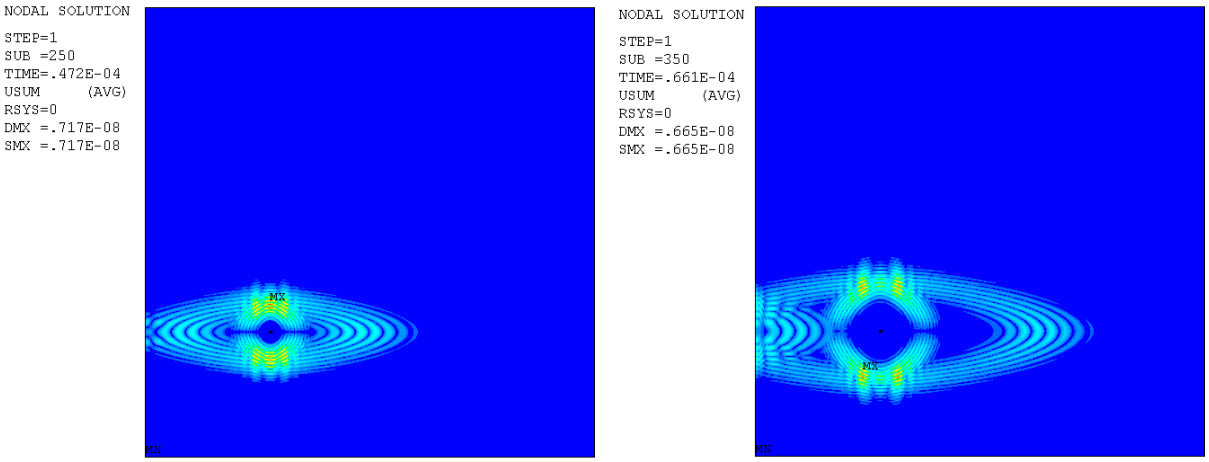

Figure 5. Propagation of the fundamental shear horizontal SH0 and the symmetric S0 wave modes in the case of $[\pm 5°]_4$ configuration for 250-th and 350-th time steps.

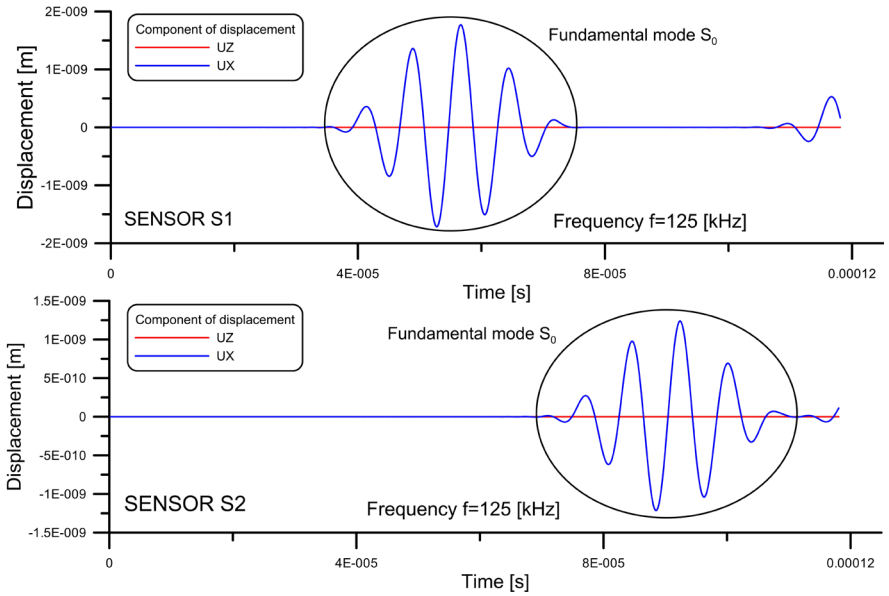

Figure 6. Dynamic response of the plate of configuration $[\pm 5^{o}]_4$ registered by sensors S1 and S2.

Table 3. Results of the identification of the fundamental elastic wave mode S0.

Laminate configuration	Envelope moment EMM		Cross-correlation CCM	
	Group velocity c_g^{EM} [km/s]	Relative error $\lvert c_g^{EM} - c_g\rvert/c_g$ [%]	Group velocity c_g^{EM} [km/s]	Relative error $\lvert c_g^{EM} - c_g\rvert/c_g$ [%]
$[\pm 5°]_4$	10.698	1.094	10.641	0.559
$[\pm 15°]_4$	10.118	1.127	10.065	0.592
$[\pm 25°]_4$	9.133	2.277	8.988	0.653
$[\pm 35°]_4$	7.663	2.151	7.581	1.064
$[\pm 45°]_4$	6.117	3.261	6.019	1.060
$[\pm 55°]_4$	4.781	6.404	4.578	10.377
$[\pm 65°]_4$				
$[\pm 75°]_4$	No possibility of identification of the fundamental wave mode S0			
$[\pm 85°]_4$				

Figure 7 represents the considered composite plate with the geometrical dimensions and the position of the actuator and sensors in the case of the second variant of simulation, where the fundamental shear horizontal mode is identified. This picture also shows the schema of the actuator and the way how the elastic wave is excited. The values of the variable geometrical dimensions with respect to the laminate configuration are collected in Tab. 4, where there are shown only these laminate configurations for which the fundamental shear horizontal wave mode SH0 identification is possible.

The proposed model of the actuator A1 acts in the following way. In the direction, which is parallel to the *X*-axis of the global coordinate system the fundamental symmetric wave mode S0 is excited. However, in the direction which is parallel to the Y-axis, the fundamental shear horizontal wave mode SH0 is to be expected. Therefore, in order to identify the SH0 modes, the component of displacement *UY* registered by the sensors S1 and S2 are analysed. As before, the pair of actuators are installed on both surfaces of the plate. Moreover, each of the actuators is modelled with the use of four solid elements of dimensions identical to the shell elements, which create the composite plate. Now the only parameter, which is identical for all simulations is the time step size $\Delta t = 3.5 \cdot 10^{-7}$ s. The appropriate wavelengths λ_{SH0} and total times of simulations t_c are presented in Tab. 5.

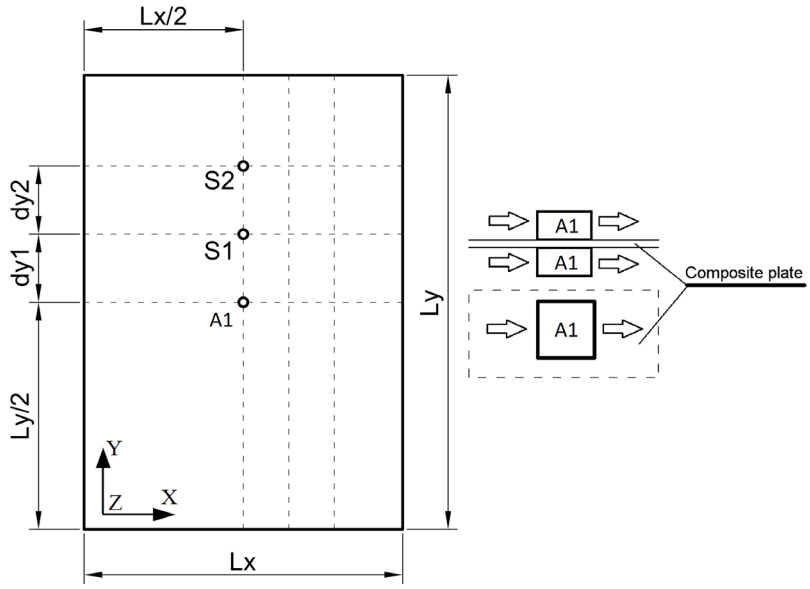

Figure 7. Model of the composite plate used for the simulation of the fundamental shear horizontal wave mode SH0: the geometrical dimensions with the location of the sensors and the schematic view of the actuator and the way how symmetric wave mode S0 is excited.

Table 4. Geometrical dimensions of the studied composite plates.

Laminate configuration	Plate		Element size l_e [mm]	$dy1$ [mm]	$dy2$ [mm]
	Lx [mm]	Ly [mm]			
$[\pm 55°]_4$	700	1000	2.0	100	100
$[\pm 65°]_4$	500	1000	2.0	50	100
$[\pm 75°]_4$	450	1500	1.5	50	100
$[\pm 85°]_4$	450	1500	1.5	50	100

Table 5. Geometrical dimensions of the studied composite plates.

Laminate configuration	Wavelength λ_{SH0} [mm]	Total time of simulation $t_c \cdot 10^{-4}$ [s]	Number of time steps n_t
$[\pm 55°]_4$	40.875	0.805	230
$[\pm 65°]_4$	34.683	1.120	320
$[\pm 75°]_4$	25.972	1.190	340
$[\pm 85°]_4$	18.259	1.190	340

The exemplary pattern of resultant displacement for the laminate configuration $[\pm 75°]_4$ is shown in Fig. 8, where there are presented the results obtained for 150, 200, 250, and 300 time steps of the simulation. A clearly visible ring around the actuator is the fundamental shear horizontal elastic wave mode SH0. In this picture, there is also visible the fundamental symmetric wave mode S0. Unfortunately, together with decreasing value of the fibre orientation angle θ, the pattern of the propagating fundamental wave modes changes dramatically. In Figure 9, there is shown the pattern of the resultant displacement obtained for 100, 150, 200, and 250 time steps of the simulation for composite configuration $[\pm 65°]_4$.

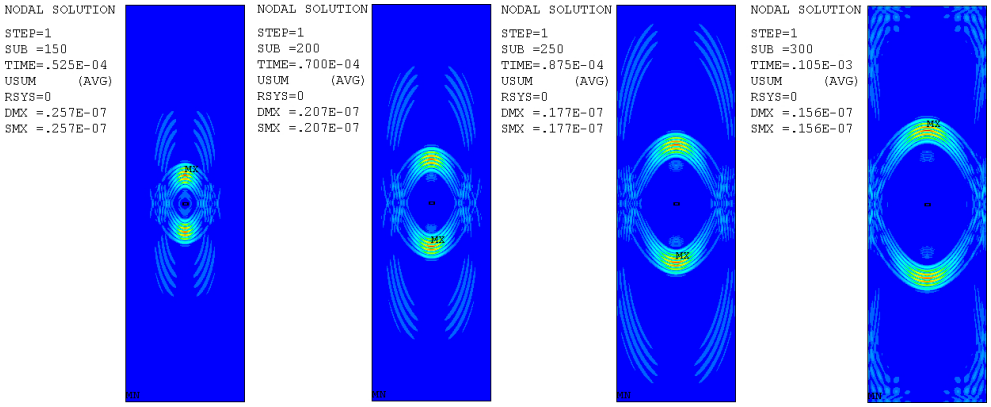

Figure 8. Propagation of the fundamental shear horizontal SH0 and symmetric S0 wave modes in the case of $[\pm 75°]_4$ configuration for 150, 200, ..., 300 time steps.

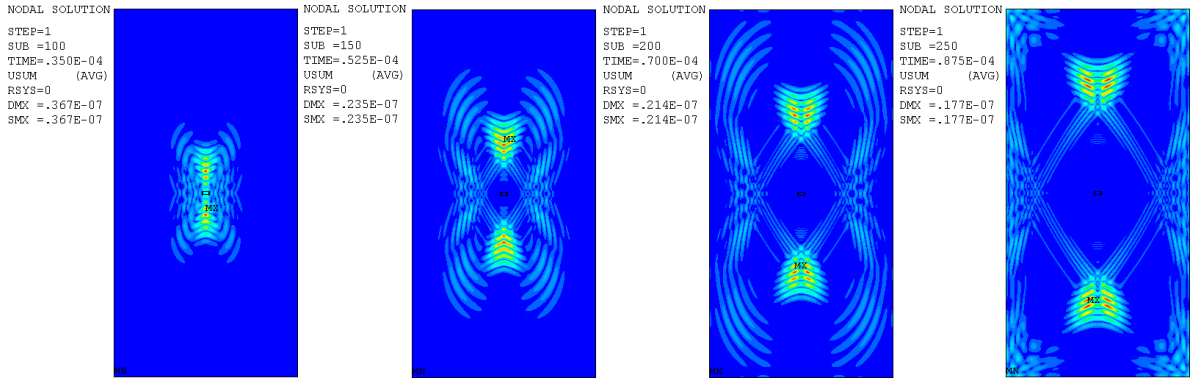

Figure 9. Propagation of the fundamental shear horizontal SH0 and symmetric S0 wave modes in the case of $[\pm 65°]_4$ configuration for 100, 150, ... , 250 time steps.

As the consequence of the interaction between the present wave modes, the results of the estimation of the group velocity c_g are getting worse, and the relative error increases (Tab. 6). The last laminate configuration, for which the estimation of the group velocity could be done, is $[\pm 55°]_4$. However, it should be stressed that this estimation should be concerned as not reliable although the obtained value of relative error is not very high (Tab. 6).

Table 6. Results of the identification of the fundamental elastic wave mode SH0.

Laminate configuration	Envelope moment EMM		Cross-correlation CCM	
	Group velocity c_g^{EM} [km/s]	Relative error $\lvert c_g^{EM} - c_g\rvert / c_g$ [%]	Group velocity c_g^{EM} [km/s]	Relative error $\lvert c_g^{EM} - c_g\rvert / c_g$ [%]
$[\pm 55°]_4$	–	–	5.102	0.343
$[\pm 65°]_4$	4.535	5.351	4.202	2.395
$[\pm 75°]_4$	3.322	3.212	3.284	2.026
$[\pm 85°]_4$	2.361	3.737	2.323	2.050

4. Conclusions

It should be stressed here that in the case of simulations of the fundamental symmetric and the shear horizontal elastic wave modes S0 and SH0 the input signals are excited with the use of cubic-shaped models of actuators. This model of actuators causes that together with the symmetric wave mode S0 the shear horizontal wave mode SH0 is also excited. Therefore, for the fibre orientation angle $\theta > 45°$ in the case of simulation of the symmetric wave mode S0, it is very difficult or even impossible to distinguish between these modes. For the other values of the angle θ the fundamental elastic wave modes are identified with relatively high precision.

Additional information

The author(s) declare: no competing financial interests and that all material taken from other sources (including their own published works) is clearly cited and that appropriate permits are obtained.

References

1. S. Zhongqing, Y. Lin; Identification of damage using Lamb waves; Springer-Verlag, 2009
2. Z. Su, L. Ye, Y. Lu; Guided Lamb waves for identification of damage in composite structures; J. Sound Vib., 2006, 295, 753-780
3. M. Barski, A. Stawiarski; The crack detection and evaluation by elastic wave propagation in open hole structures for aerospace application; Aerosp. Sci. Technol., 2018, 81, 141-156
4. W.T. Thompson; Transmission of elastic waves through a stratified solid medium; J. Appl. Phys., 1950, 21(2), 89-93
5. N. Haskell; Dispersion of surface waves on multilayered media; B Seismol. Soc. Am., 1953, 43, 17-34
6. A.H. Nayfeh; The general problem of elastic wave propagation in multilayered anisotropic media; J. Acoust. Soc. Am., 1991, 89(4), 1521-1531
7. M.A. Hawwa, A.H. Nayfeh; The general problem of thermoelastic waves in anisotropic periodically laminated composites; Compos. Eng., 1995, 5(12), 1499-1517
8. L.A. Konopoff; Matrix method for elastic wave problems; B Seismol. Soc. Am., 1964, 43, 431-438
9. L. Wang, S.I. Rokhlin; Stable reformulation of transfer matrix method for wave propagation in layered anisotropic media; Ultrasonics, 2001, 39, 413-424
10. S.I. Rokhlin, L. Wang; Stable recursive algorithm for elastic wave propagation in layered anisotropic media: Stiffness matrix method; J. Acoust Soc Am., 2002, 112(3), 822-834
11. M. Barski, P. Pająk; Determination of Dispersion Curves for Composite Materials with the use of Stiffness Matrix Method; Acta Mechanica et Automatica, 2017, 11(2), 121-128
12. M. Barski, A. Muc, A. Stawiarski; The influence of the configuration of the fiber-metal laminates on the dispersion relations of the elastic wave modes; Vibrations in Physical Systems, 2020, 31(2), 2020202; DOI: 10.21008/j.0860-6897.2020.2.02
13. A. Muc, M. Barski, A. Stawiarski, M. Chwał, M. Augustyn; Dispersion curves and identification of elastic wave modes for fiber metal laminates; Compos. Struct., 2021, 255; DOI: 10.1016/j.compstruct.2020.112930.
14. F. Moser, L.J. Jacobs, J. Qu; Modelling elastic wave propagation in waveguides with the finite element method; NDT&E International, 1999, 32, 225-234
15. D. Cerniglia, A. Pantano, N. Montinaro; 3D simulations and experiments of guided wave propagation in adhesively bonded multi-layered structures; NDT&E International, 2010, 43, 527-535
16. C. Willberg, S. Duczek, P.J. M. Vivar, D. Schmicker, U. Gabbert; Comparison of different higher order finite element schemes for the simulation of Lamb waves; Comput. Methods Appl. Mech. Eng., 2012, 241-244, 246-261
17. P. Kudela, A. Żak, M. Krawczuk, W. Ostachowicz; Modelling of wave propagation in composite plates using the time domain spectral element method; J. Sound Vib., 2007, 302(4-5), 728-745
18. W.M. Ostachowicz; Damage detection of structures using spectral finite element method; Computers & Structures, 2008, 86(3-5), 454-462